Electrodeless plasma thrusters and magnetized plasma expansions for space propulsion

Mario Merino, Jaume Navarro-Cavallé, Pablo Fajardo, Marco Inchingolo, Pedro Jiménez, Jiewei Zhou, Diego García-Lahuerta, Célian Boyé, Davide Maddaloni, Filippo Terragni, Eduardo Ahedo

75th Annual Gaseous Electronics Conference
October 3 - 7, 2022 Sendai, Japan

Contents

Electrodeless plasma thrusters

- Electrodeless plasma thrusters (EPTs) aim at higher flexibility, simplicity, scalability and durability than current technologies (e.g. Hall thrusters) thanks to:
  1. Electromagnetic waves (in the MHz-GHz range) to energize the electrons in the plasma
  2. An applied magnetic field to expand and accelerate the resulting plasma to high velocities (Magnetic Nozzle)

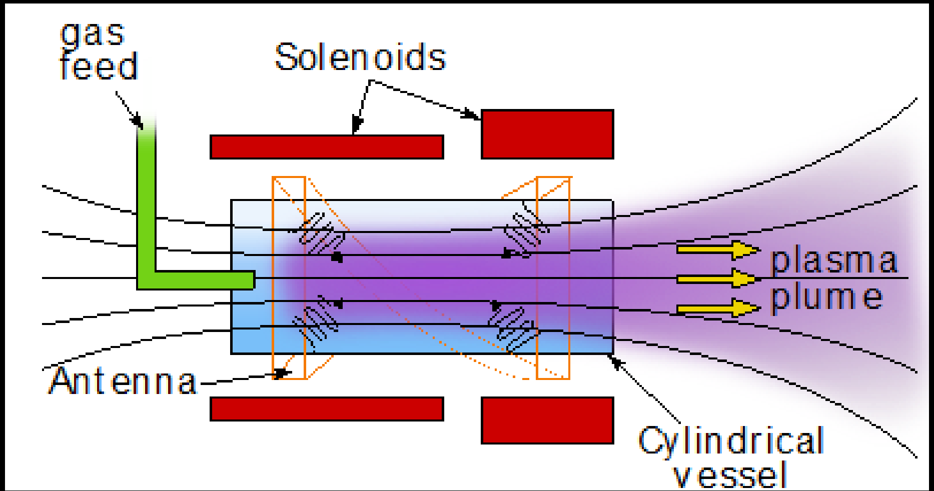

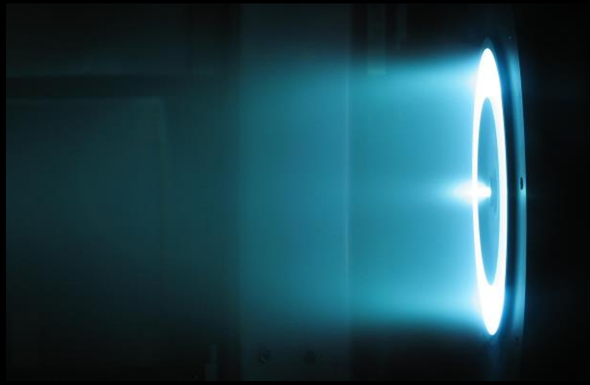

Hall effect thruster

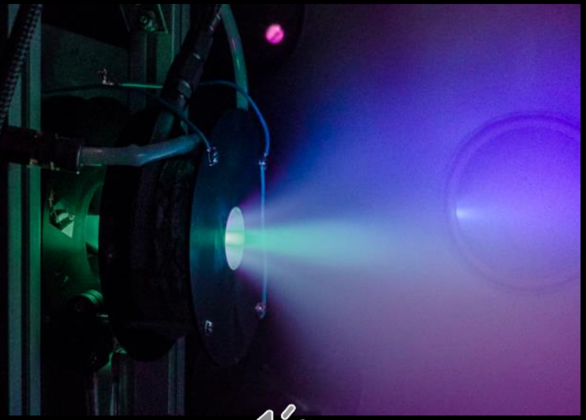

Helicon plasma thruster

- EPT performance is still poor: Physics are still not well understood
  - Plasma-wave interaction and effects of the EM fields on plasma transport
  - Mechanisms that explain the high losses to the walls still unknown
  - External expansion in the diverging magnetic nozzle: kinetic behavior of the near-collisionless electrons

ELECTRON CYCLOTRON RESONANCE THRUSTER

COAXIAL THRUSTER DESIGN (ONERA)

- TEM wave mode propagation requires an electrode in the plasma chamber.
  - Not truly electrodeless
- Power range 30-200W at 2.45 GHz
- Reported thrust efficiency up to 16% [1]
- Central conductor suffers erosion
- Nearly 10 years of development

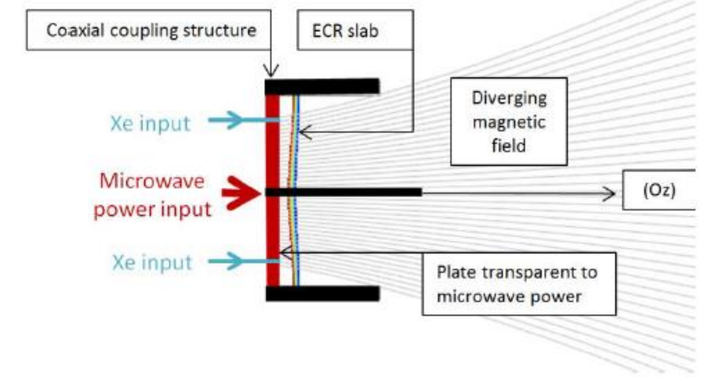

[1] Cannat, F., et al. "Optimization of a coaxial electron cyclotron resonance plasma thruster with an analytical model." Physics of Plasmas 22.5 (2015): 053503.

WAVEGUIDE THRUSTER DESIGN (EP2 new development)

- TE11 wave mode propagation (simple circular waveguide)
- Truly electrodeless
- Modular approach for easy design iterations.
- 5.8GHz microwaves for smaller plasma chamber, low power and mass flow rate requirements.
- Magnetic field generator: permanent magnet (PM) + electromagnet (EM) for resonance position tuning and nozzle divergence control.

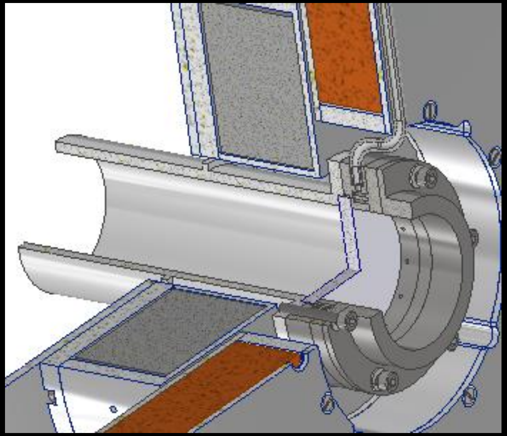

Plasma Chamber Dimensions: Radius, Length	18mm, 20mm
Microwave Power	50-300 W
Mass flow rate (Xe)	1-40sccm
MW frequency	5.8 GHz
B resonance	2070 G
Magnet type	Sm-Co YXG-32
Max electromagnet power	500 W
Electromagnet max B field	900G

[2] Inchingolo M, Navarro-Cavallé J. and Merino M. "Direct thrust measurements of a circular waveguide electron cyclotron resonance thruster", (IEPC-2022-338)

Waveguide ECRT Results

- First plume and direct thrust measurements have been performed.
- Thrust of 3.5 mN and Thrust efficiencies up to 4% have been measured
- Main limitation coming from relatively low electron temperature and consequently low ion acceleration ($T_e = 4 - 20$ eV, $E_i = 50 - 120$ eV)
- Plume Ion current measurements present two peaks appear at large angles for low powers → “Hollow plume” (with large divergence)
- Reflected power is not negligible and depends on the mass flow rate and input power (10–50%).
  - This confirms the expectation that the thruster input impedance is being affected by the plasma conditions.

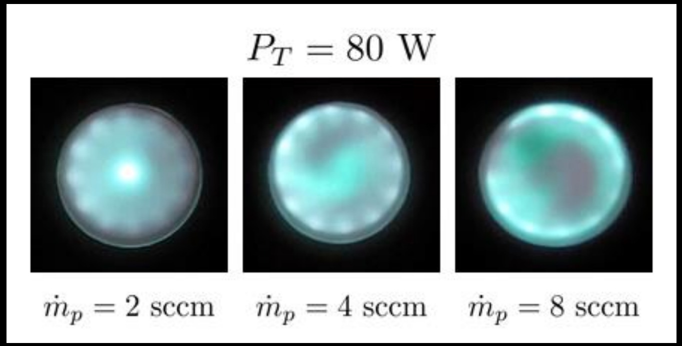

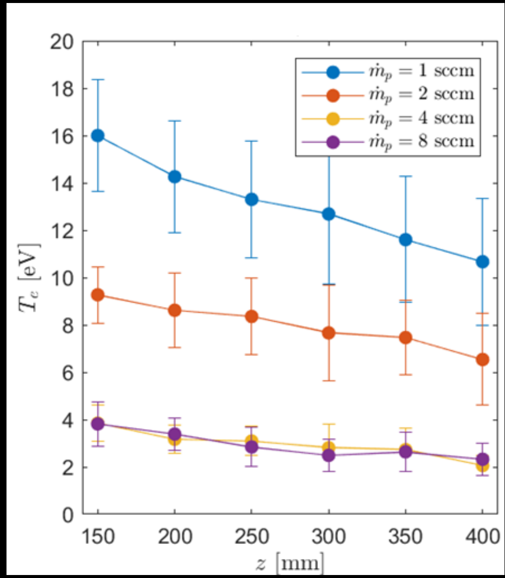

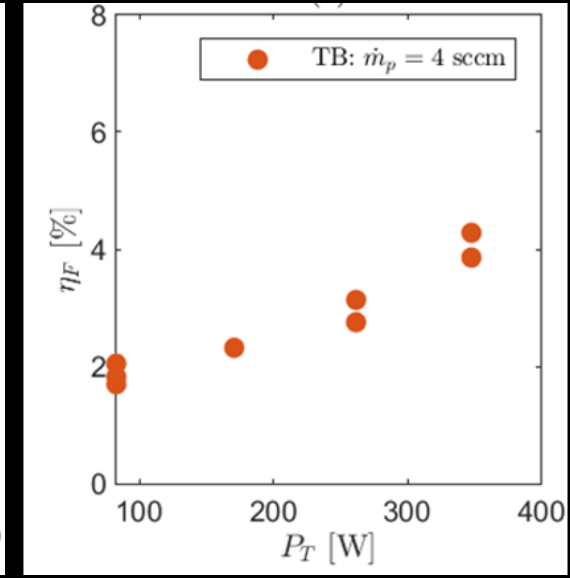

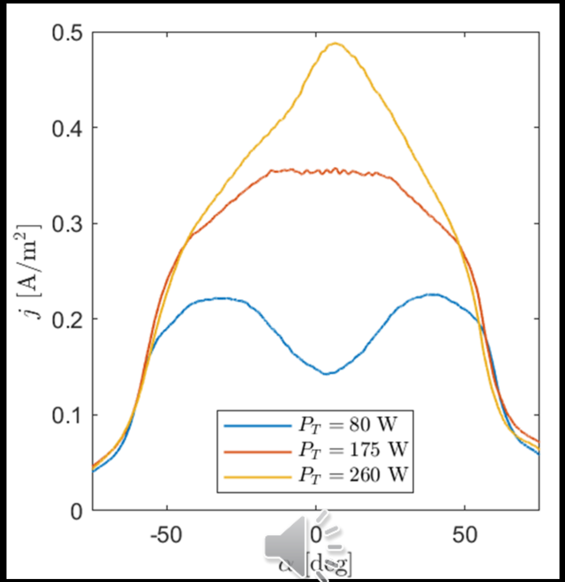

[2] Inchingolo M, Navarro-Cavallé J. and Merino M. “Direct thrust measurements of a circular waveguide electron cyclotron resonance thruster”, (IEPC-2022-338)

Simulation of ECRTs

- Hybrid PIC/fluid (HYPHEN code) + wave simulation of Coaxial ECRT at ONERA
  - Cold plasma dielectric tensor model used for waves; power deposition map updated until steady-state convergence is reached
- Multiple wave transitions exist in the thruster chamber and near plume, not just the ECR. Meshing is adapted accordingly to the local wavelength
- Absorbed power concentrates about the ECR and the length of the inner rod. Minor additional absorption also observed at the UHR downstream
- Large T_e gradient and associated density cavity observed

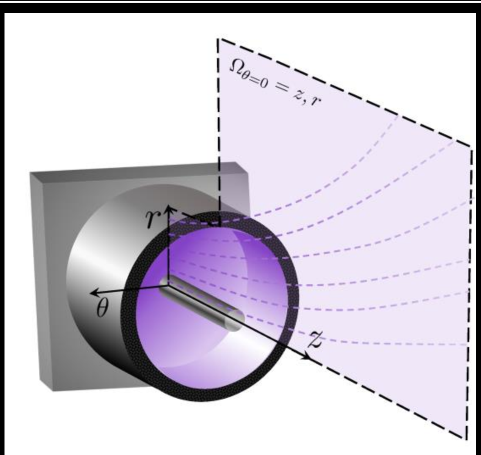

[Álvaro Sánchez-Villar et al, Plasma Sources Sci. Technol. 30 (2021) 045005]

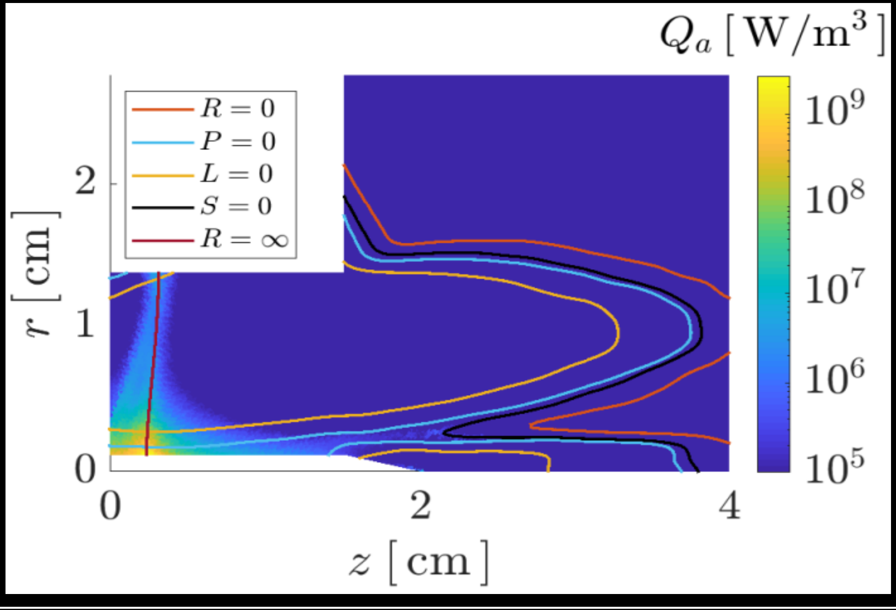

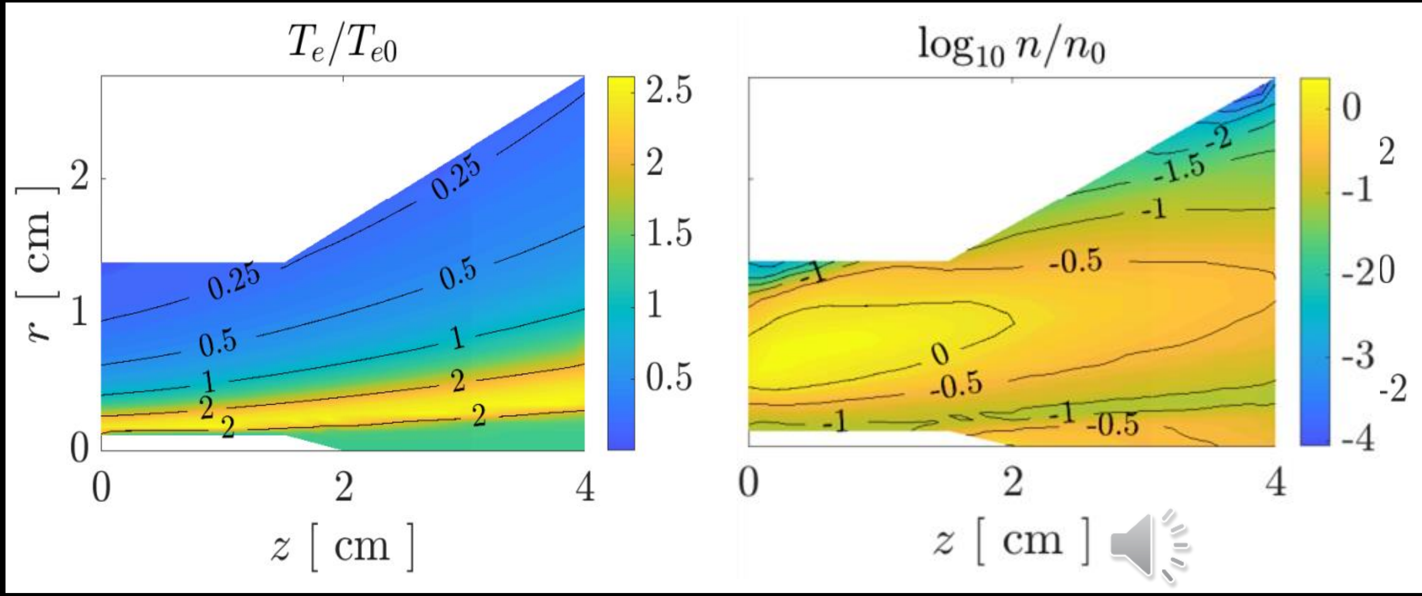

Simulation of ECRTs

- Recent comparison against experimental data from ONERA partially validates the code:
  - Overall good agreement on normalized current, density, and potential profiles
  - Numerical results are sensitive to the ad-hoc anomalous transport model used, with one free parameter used for data fitting (borrowed from HET modeling).

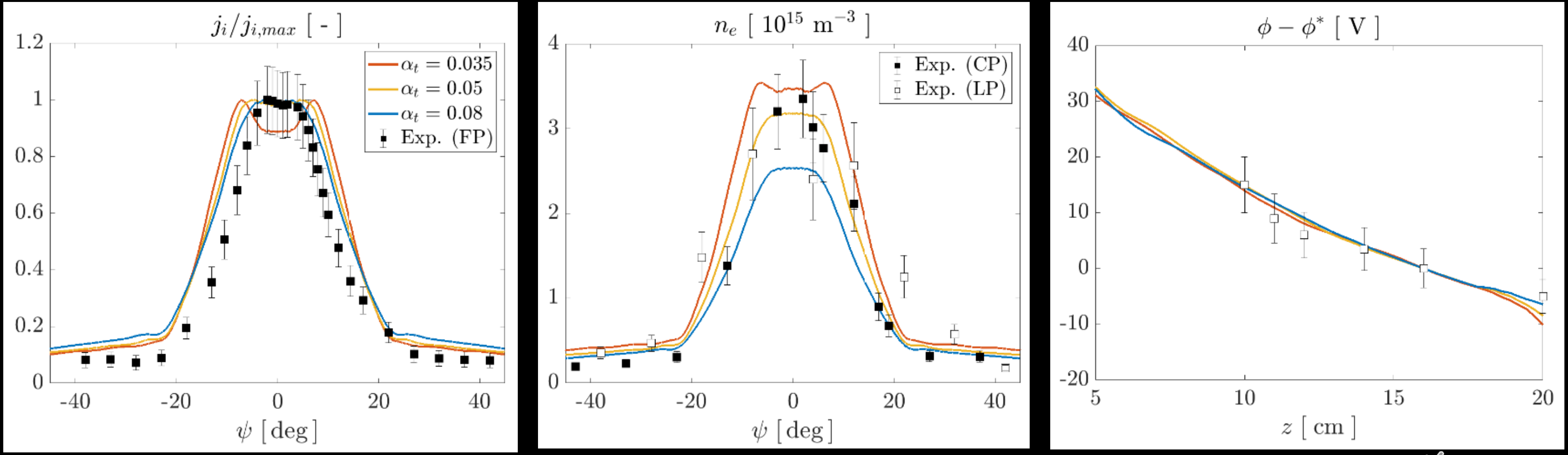

Helicon Plasma Thruster development

- Development of different prototypes in the last 6 years
  - Magnetic field generator: Electromagnets/PM based
  - Different antenna geometries have been testes: simple/double loops, half helical.
  - RF power (13.56 MHz) : 300 – 700 W
  - 3-10 mN, 2 % efficiency (low performance)

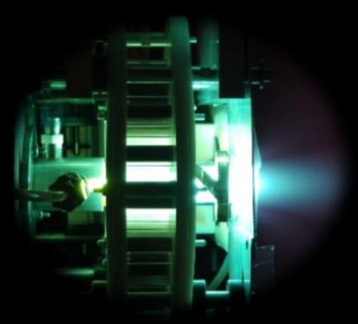

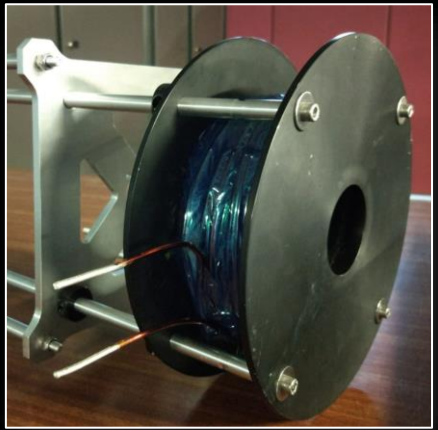

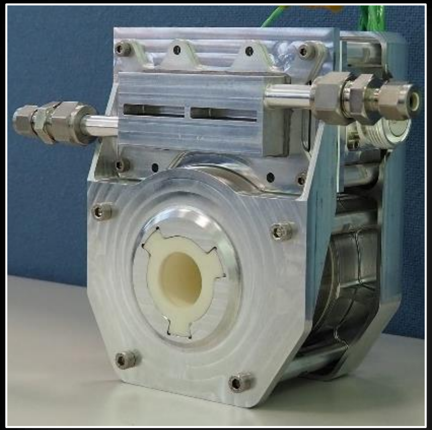

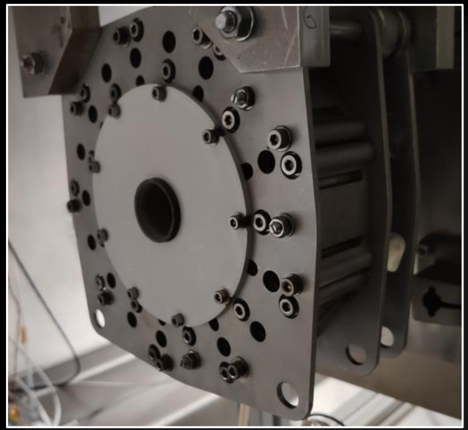

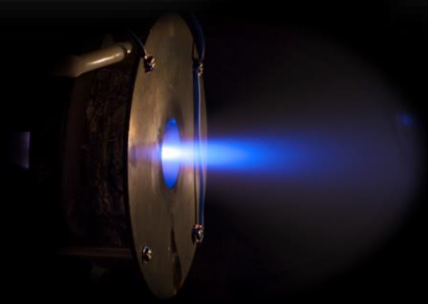

Helicon Plasma Thruster simulations (PM prototype)

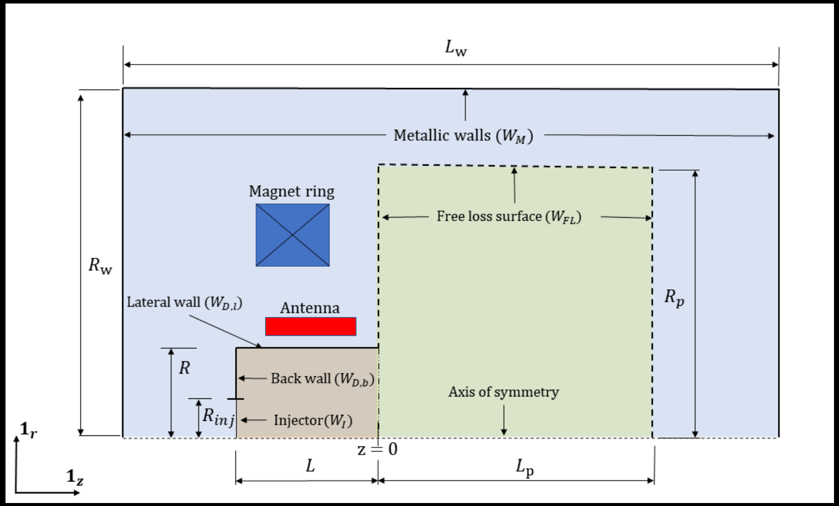

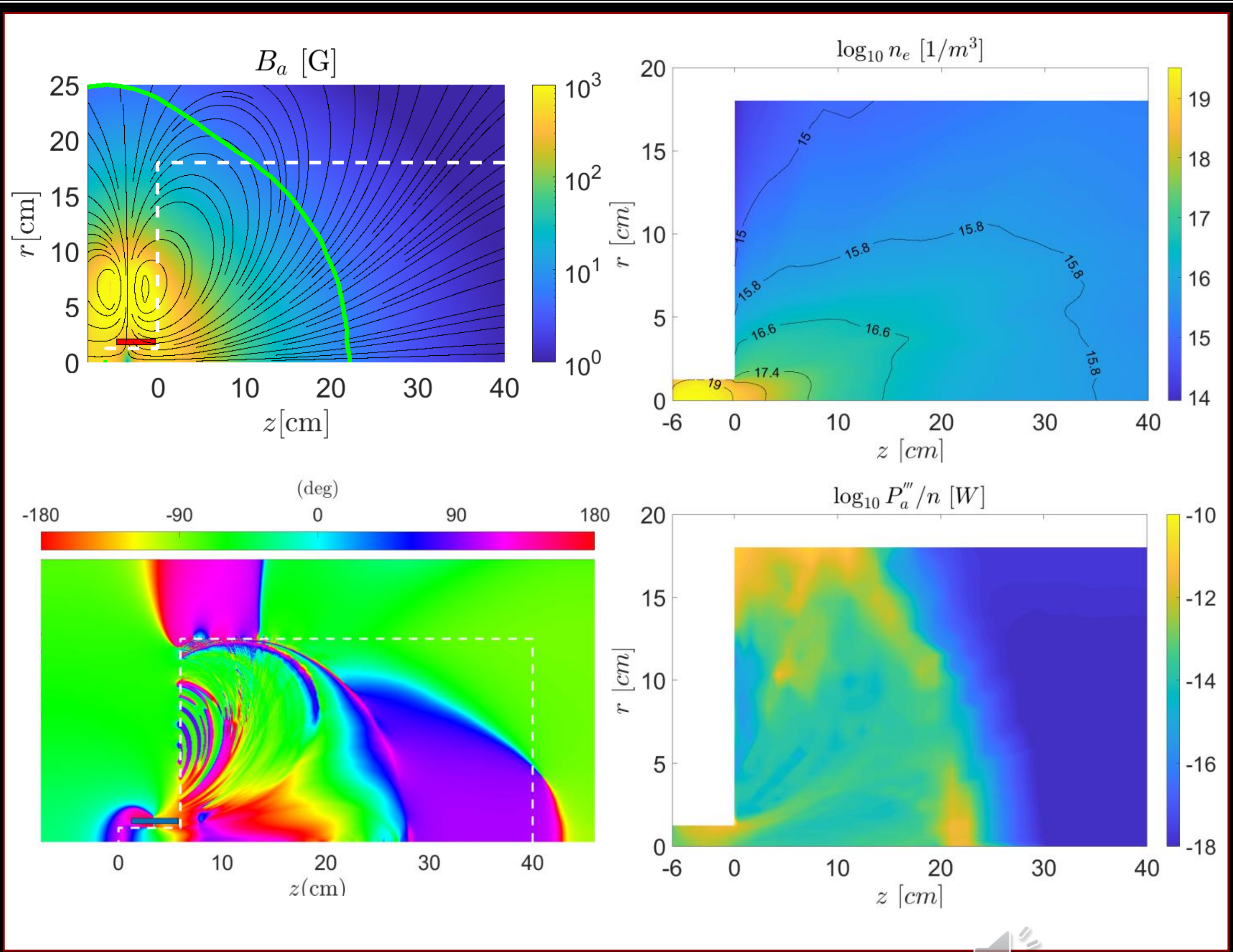

- Power deposition *per particle* is largest inside the source and at the ECR that always exist downstream
- Large losses at the cusp-like field in the chamber

Electron kinetics in a MN

- Many aspects of the near-collisionless expansion in a MN cannot be studied with fluid models, in particular the electron collective behavior:
  - Collisionless cooling
  - Anisotropization
- In steady state, the collisionless, fully-magnetized parallel motion of individual electrons follows an effective potential:

$$E + \underbrace{e\phi(s) - \mu B(s)}_{U_{eff}\text{, effective potential}} = 0$$

- Depending on their energy E and magnetic moment μ, turning points allow classifying electrons as
  - Free electrons (escape to ∞)
  - Reflected electrons (back to the source)
  - Trapped electrons (trajectories do not connect neither with the source nor infinity)

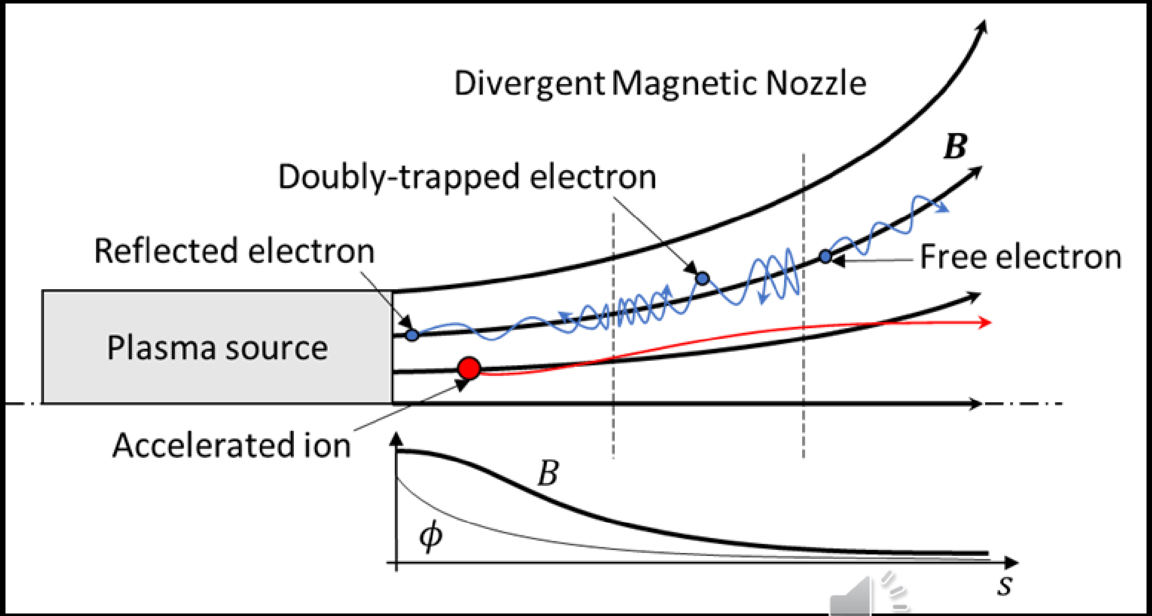

Kinetic electron model

- A semi-analytical kinetic model of the 1D2V motion of electrons along the magnetic tubes can be set up [Phys Plasmas 22, 053501 (2015)], [Plasma Sources Sci. Technol. 30 (2021) 115006]
  - Main assumptions: steady state, collisionless, fully magnetized electron motion, quasineutral plasma
- Electron motion conserves mechanical energy E and magnetic moment μ, and the gyroaveraged distribution function $f_e(s, E, \mu)$ satisfies

$$v_{\parallel} \frac{\partial f_e}{\partial s} = 0$$

  - $f_e(s, E, \mu)$ is constant along each magnetic line (s) as long as $v_{\parallel} \neq 0$
  - We fix a semi-Maxwellian electron distribution upstream, and compute all free and reflectd electrons this way
  - Trapped electrons depend on the transient plume set up process, collisions, and/or instabilities.
    - Here, we assume the same distribution as upstream is valid for trapped electrons

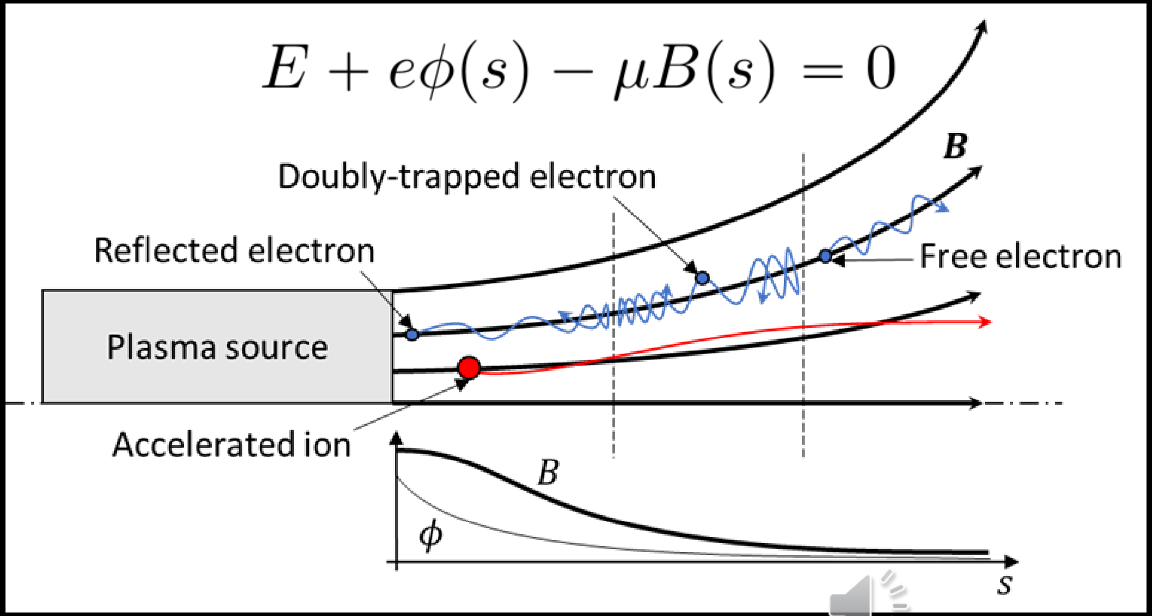

Kinetic electron response

- Reflected electrons dominate at the beginning of the expansion
- Doubly-trapped electrons dominate soon afterward
- Free electrons are a minority, but give rise to all odd-moments of f_e (e.g. bulk velocity)
- Electrons exhibit collisionless cooling and develop anisotropy downstream
- This behavior is missed by simple polytropic models

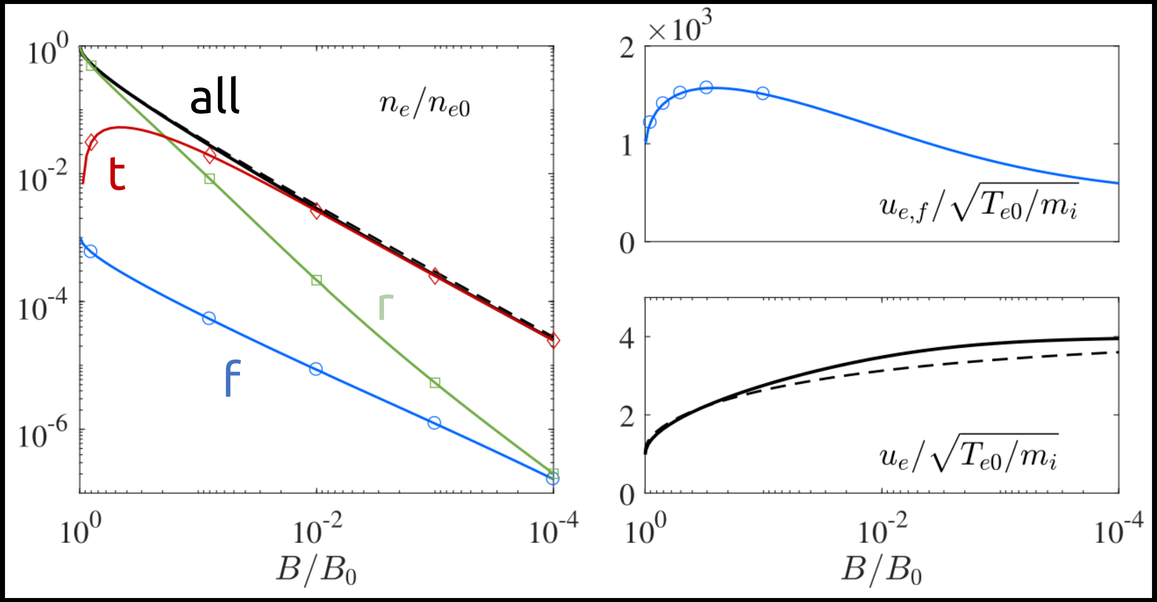

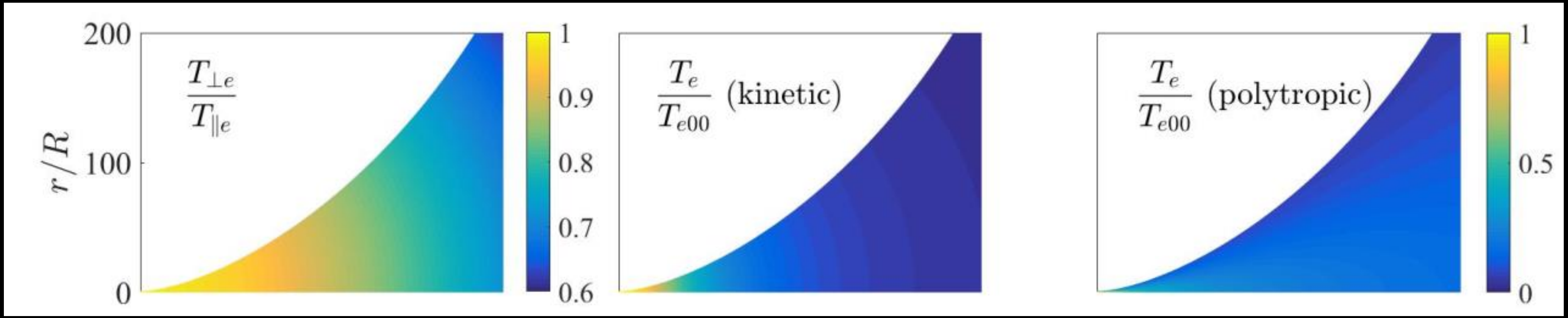

Kinetic electron response

- Electric potential ϕ with the kinetic electrons goes to a well-defined asymptote, ϕ_∞
- This value controls the net electron current to infinity, given by the free electrons, while it does not affect the net ion current
    - For a globally current free MN, this value is given by the ion current extracted from the source
- The approximate polytropic model with same ϕ_∞ approaches this value at a lower rate. Differences are important in the major part of the expansion
- Electric potential map differs from simpler, but unjustified, fluid models. The actual potential map is a key aspect for plume-spacecraft interaction

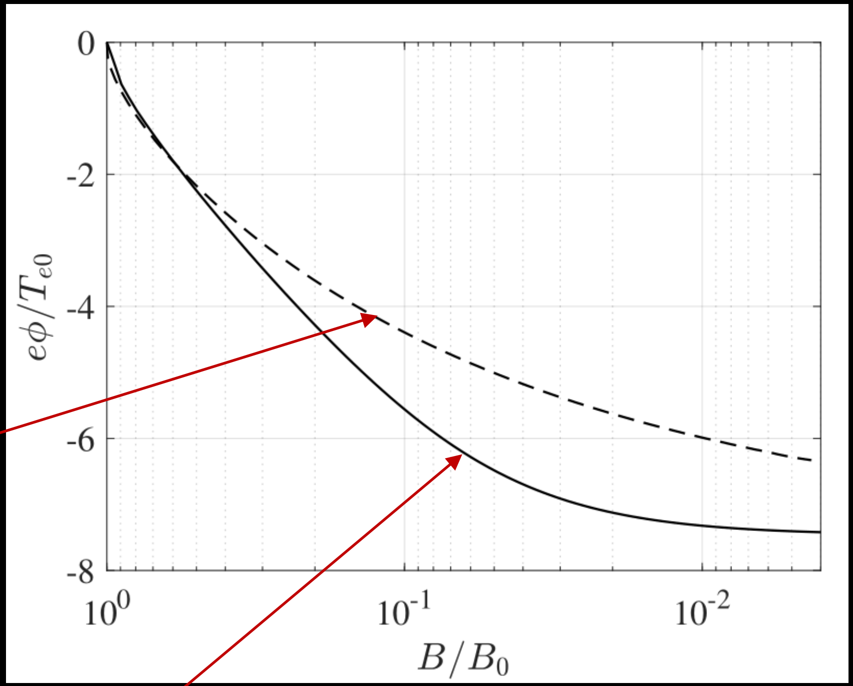

Polytropic $\gamma = 1.155$

kinetic model

Azimuthal oscillations in Magnetic Nozzles

- The FFT of two synced probes can be used to resolve the dispersion diagram (see previous work by Hepner et al, Appl. Phys. Lett. 116, 263502 (2020)):

$$k(\omega) = \frac{\Delta\theta(\omega)}{d}$$

  - Multiple realizations are needed to average out noise
  - This can be done e.g. for the floating potential or the ion saturation current
- The plume of the permanent-magnet HPT is studied in this manner to reveal azimuthal oscillations

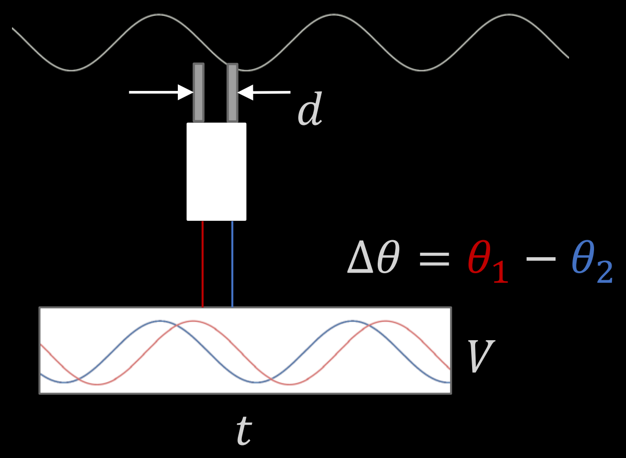

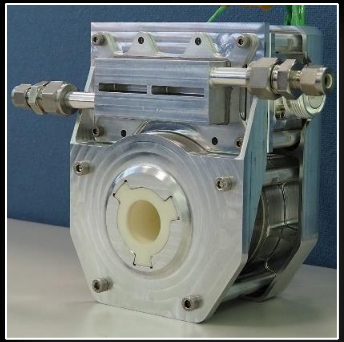

  - Different spectra in the 10s of kHz is seen in the floating potential at the center of the plume and its periphery
    - Low f oscillations (axial?)
    - moderate f azimuthal oscillations

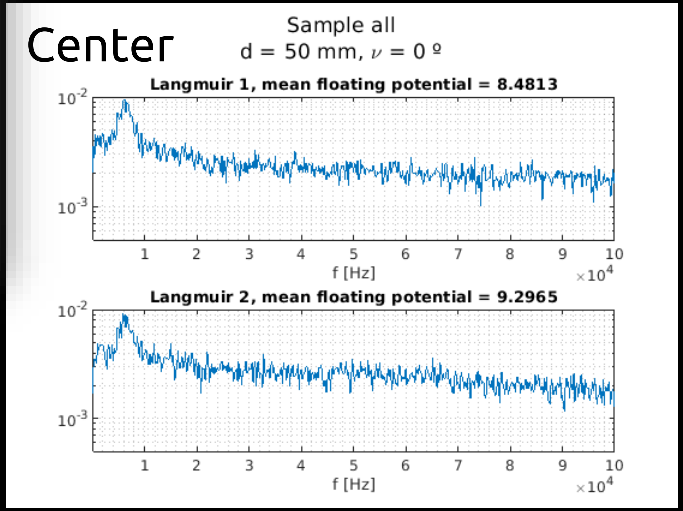

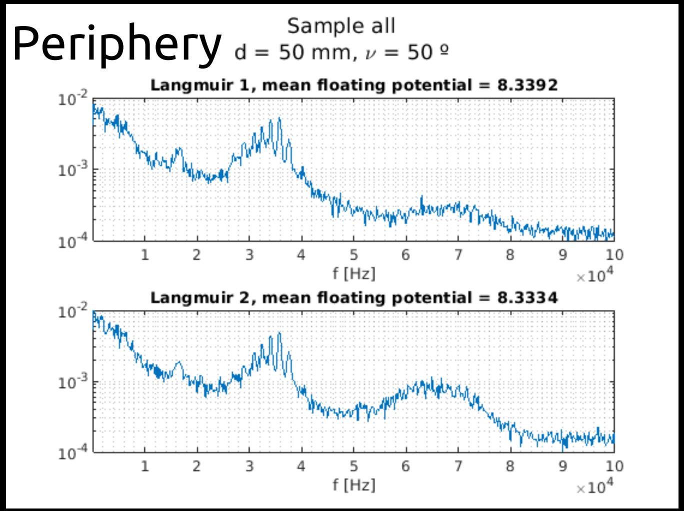

AZIMUTHAL OSCILLATIONS IN MAGNETIC NOZZLES

- The reconstructed dispersion diagrams show
  - A $k_\theta = 0$ oscillation at low frequencies (< 10 kHz) at all three polar angles sampled
  - A dispersion relation with $k_\theta(\omega) \neq 0$ outside of the plume centerline, extending up to about 100 kHz
    - Slope is dependent on polar angle, as expected for azimuthal modes
  - Stronger oscillations along this branch at specific ω, k_θ ranges, likely integer azimuthal m modes
- Assessment of these oscillations is still ongoing, but likely drift-like oscillations

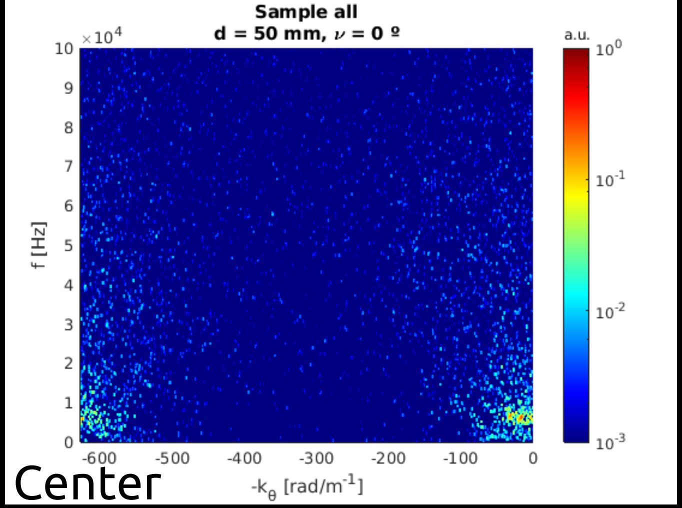

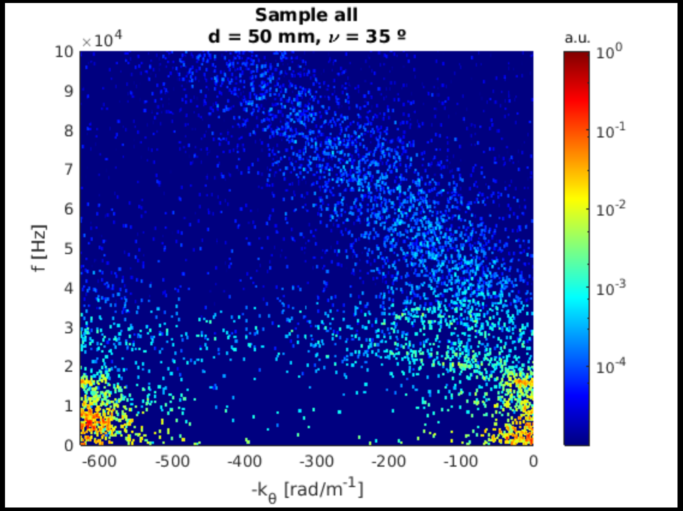

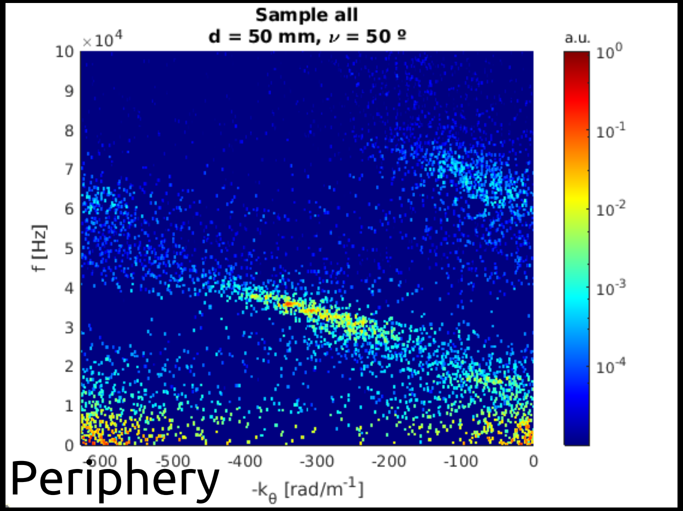

- Ongoing work at EP2: using 4 probes it is possible to resolve the wavenumber <u>vector</u>

Plasma acceleration in a Magnetic arch

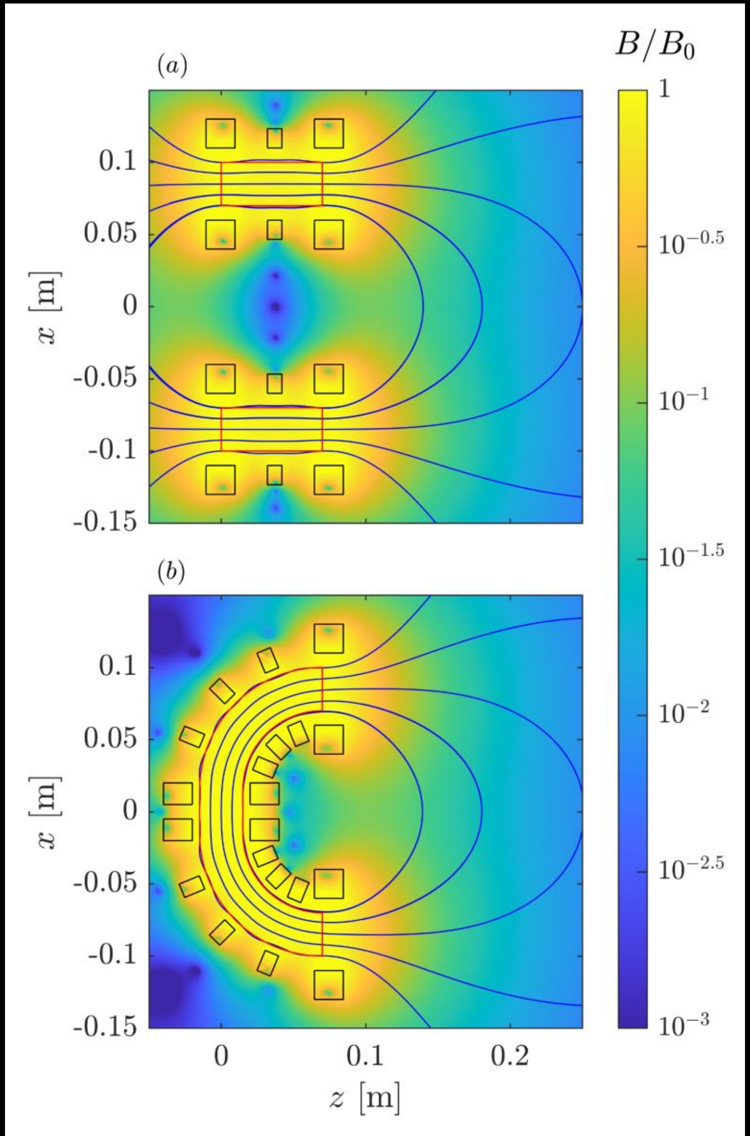

- When two cylindrical EPTs with opposing polarities are flown side by side (for zero magnetic torque on the platform) their MNs connect and form a **magnetic arch**
- This magnetic topology differs from an axisymmetric MN
  - It is fully 3D
  - The two beamlets interact and may form shock-like structures
  - Applied field lines are essentially ⊥ to the flow downstream
- The novel Magnetic Arch thruster concept also uses a magnetic arch for plasma acceleration
  - Removes rear walls in cylindrical sources; all walls are now magnetically shielded

Magnetic Arch plasma model

- Two-fluid (ions, electrons) model [IEPC-2022-423]
- Quasineutral, collisionless, no induced field $\boldsymbol{B}_p$
- 2D planar (future work must deal with full 3D case)

- Ions initially accelerate as in a simple magnetic nozzle
- Oblique shock structure forms where ions from the two thruster outlets interact (at the symmetry plane).
- Ion jet is able to propagate beyond the closed magnetic tube

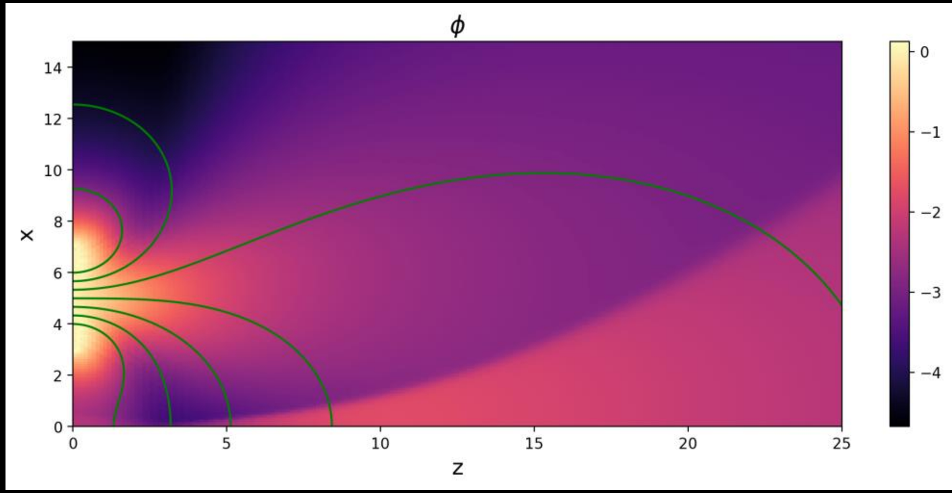

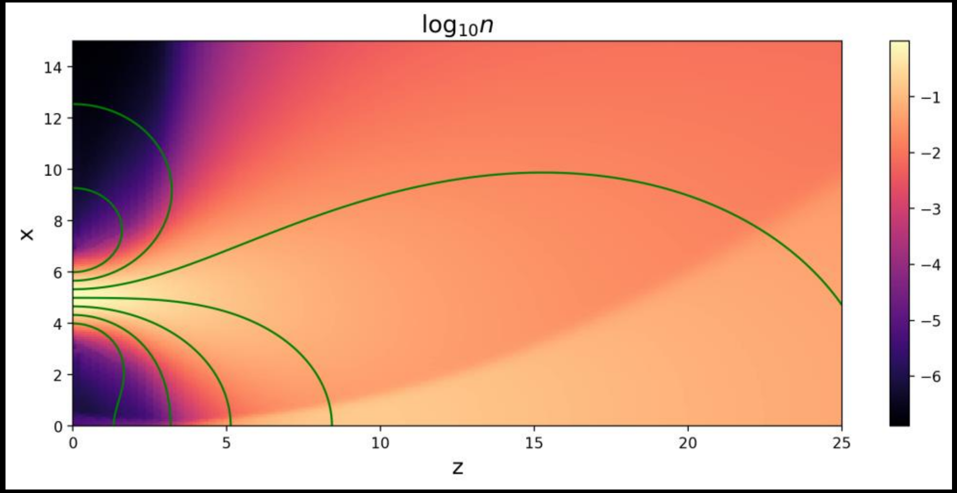

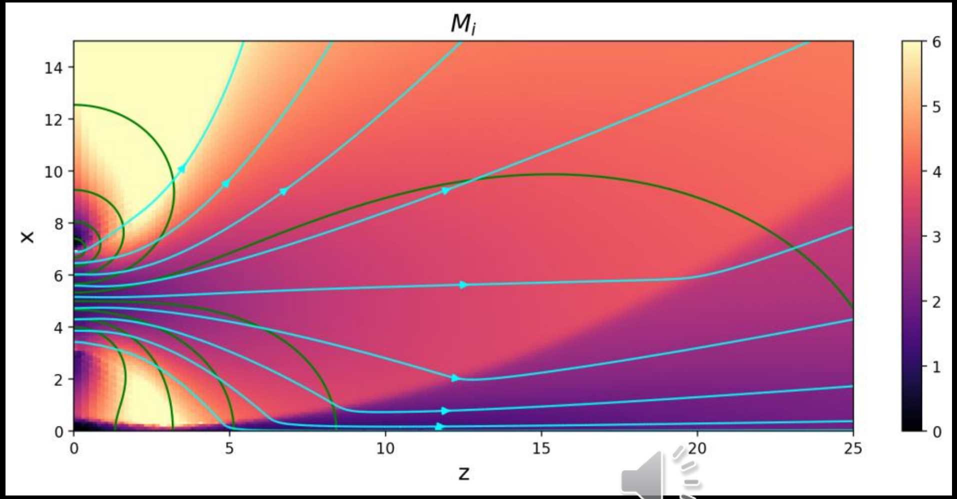

Plasma-induced Magnetic field

- From the simulation j_y we can compute the plasma-induced field $\boldsymbol{B}_p$ solving Ampère's equation with FE
  - The relevant parameter here is the plasma beta upstream β_0

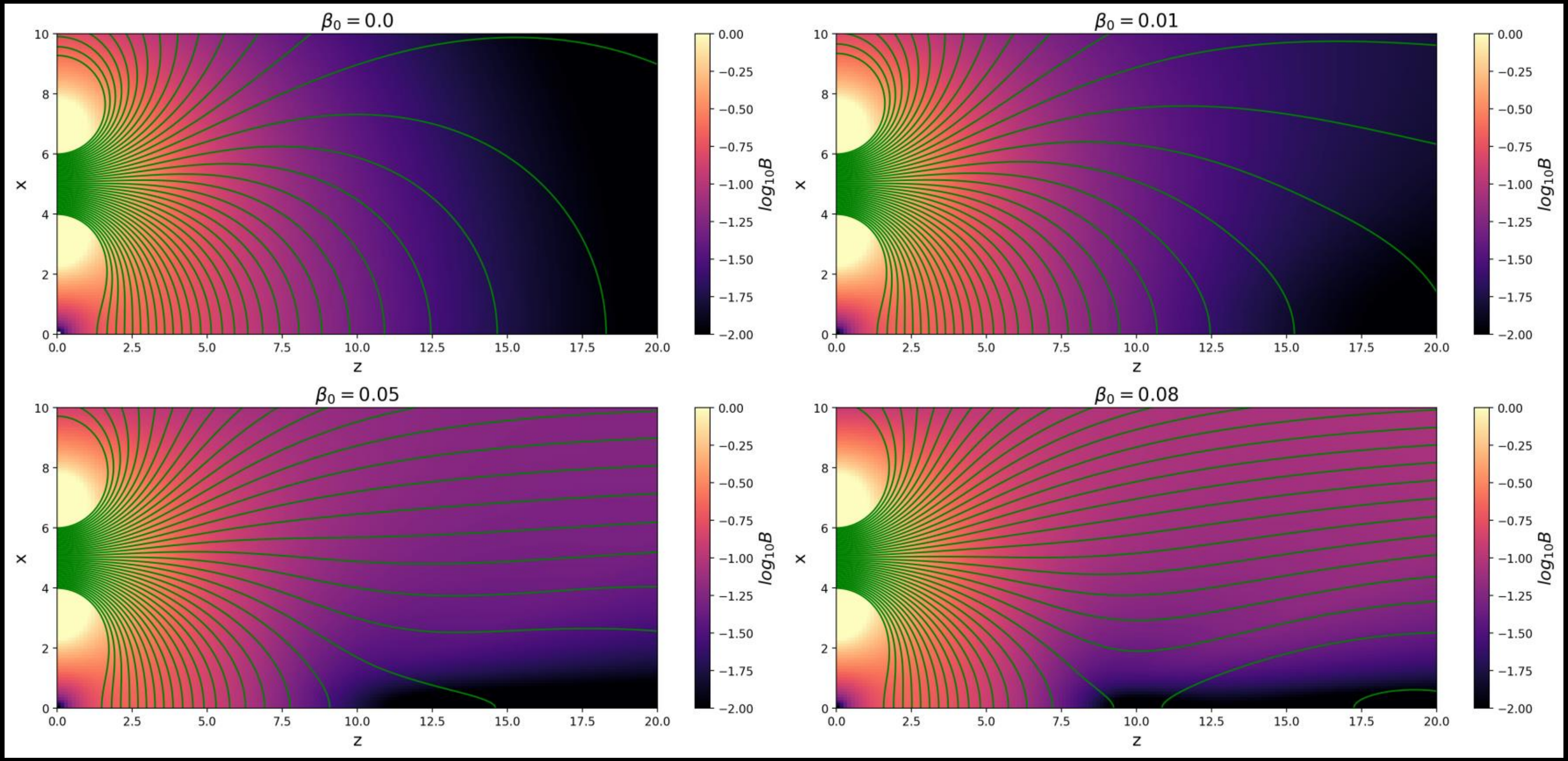

- $\boldsymbol{B}_p$ opens the lines and stretches them to infinity
- Eventually a separatrix forms
- Separate magnetic domains exist:
  - Inward closed lines
  - Outward stretched lines
  - New domain after separatrix

Acknowledgments

This project has received funding from the European Research Council (ERC) under the European Union's Horizon 2020 research and innovation programme (grant agreement No 950466)

Thanks also to other previous/ongoing projects:
EU MINOTOR, EU HIPATIA, ES ESPEOS.

Thank you!

mario.merino@uc3m.es

ZARATHUSTRA